One, two ...

Light interferometry has many advantages in the area of precision measurement and positioning. It offers high accuracy and resolution, long measuring range, up to hundreds of feet, ease of setup, the capability for making measurements having very low Abbe offset, and the ability to handle small angular displacements of the stage. This paper explains operation of the Michelson interferometer with single-frequency (DC interferometry) and two-frequency sources (heterodyne or AC interferometry). It discusses measurement errors when operating in air and vacuum, and an example application.

• *Greg Swan* •

The Michelson interferometer in Figure 1 takes a single-frequency (wavelength) light source and splits it into two measurement paths going to mirrors 1 and 2. Beams 1' and 2' reflect from the mirrors and combine into a single, collinear and coaxial beam at the beam splitter. The screen shows intensity changes of the combined beam caused by mixing, or interference, of beams 1' and 2'. In early times, a human observer carefully noted and counted intensity changes from maximum to minimum to maximum again as mirror1 or mirror2 changed position. Photodiode receivers, amplifiers and digital circuitry have taken over this task.

Author

Greg Swan works as an applications engineer for Agilent Technologies Nano Positioning Metrology Division in Santa Clara, California, USA.

www.agilent.com

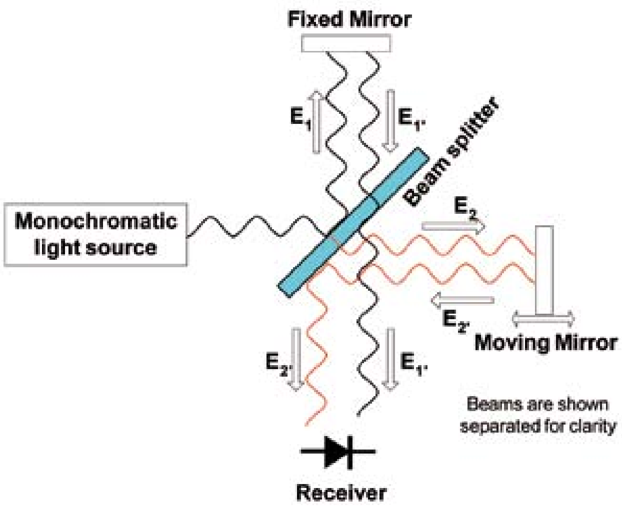

Figure 1. Michelson interferometer.

Principle

'Sine waves' shown in Figure 1 represent amplitude and phase of the electric field of a fixed-wavelength standing wave in space. Between the beam splitter and receiver, electric fields $E_{1'}$ and $E_{2'}$ add. Intensity at the screen is the magnitude of the vector sum of these fields. Assuming equal intensities of $E_{1'}$ and $E_{2'}$, a change in intensity at the screen caused by mirror motion Δd is expressed in the following equation [1]:

Michelson

$$I = 2I_0 \left[1 + \cos \left[\frac{2\pi}{\lambda} (2n\Delta d) \right] \right]$$

Ideally, $E_{1'}^2$ and $E_{2'}^2$ being constant, the intensity depends on the phase ($\theta_{1'2'}$) between the two E-fields, which is influenced by the position of the two mirrors. In Figure 1, assume the mirrors are positioned so the receiver sees the maximum intensity, meaning the two electric fields are in phase. Then we move mirror 2 to the right a distance of $\lambda/4$ or one quarter wave. This changes the phase of $E_{2'}$ by 180° because the round trip distance to mirror 2 from the beam splitter increases by $2 \cdot \lambda/4$ or one half wavelength total. The net effect is that beams $E_{1'}$ and $E_{2'}$ are 180° out of phase and when added together, they cancel each other, reducing the intensity at the receiver to zero (assuming $E_{1'} = E_{2'}$). One would say this interferometer has an Optical Fold Factor of 2, or it is a 'single-pass' interferometer configuration.

Directional uncertainty

While the mirror position is stable, the intensity at the receiver is constant. Eventually, normal use of the stage will position the mirror so light intensity at the receiver is maximum or minimum, making it difficult to know at the next sample which direction the mirror is moving, since intensity would decrease or increase respectively regardless of the direction the mirror moves. Practical DC interferometers add optics to create additional signals with different phase delays to overcome this uncertainty. The AC or heterodyne interferometer gets around this issue and will be described next.

Heterodyne

In the heterodyne interferometer, the measurement is made using two light frequencies, spaced closely together (a few MHz) relative to the light frequency ($4.7 \cdot 10^8$ MHz). Operating a helium-neon laser with an axial magnetic field splits its output into two oppositely circularly polarized frequencies (call them *f1* and *f2*) typically spaced between 1 and 7 MHz apart. This is referred to as the split frequency or Zeeman split. Optical components convert the output beam into two linear, orthogonal polarizations. Using linearly polarized light facilitates separation in the interferometer using a polarizing beam splitter. Figure 2 shows the single-pass design for conducting heterodyne interferometry.

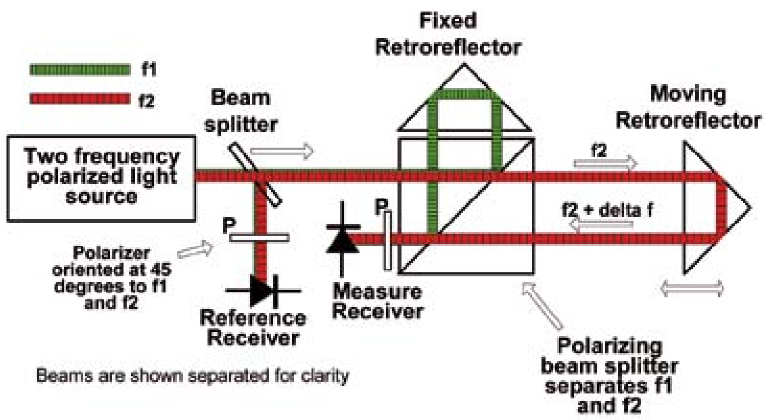

Figure 2. Heterodyne interferometer.

Replacing the beam splitter with a *polarizing* beam splitter (PBS) changes the Michelson interferometer into a modified Michelson, but it works the same way as previously described. The PBS separates and directs light from the source to two arms, but this time the light frequencies in the arms are different. Another change is replacing the mirrors with retroreflectors (which might be corner cubes). These components reflect incident light directly back toward the source, on a parallel path.

This substitution makes two improvements, helping us recover the measurement signal (a combination of *f1* and *f2*) because the retroreflector offsets the beam as shown in Figure 2, and maintains optical alignment should the stage pitch or roll. This design requires two receivers, one observes the two-frequency beam before it enters the interferometer (called the 'reference beam') and the other picks up the beam when it leaves (called the 'measure beam'). Inside each receiver, a polarizer oriented at 45° to *f1* and *f2* allows the component of *f1* and *f2* that is aligned with the polarizer axis to exit. Exiting the polarizer, the beam is linearly polarized, with the electric fields of *f1* and *f2* parallel. They interfere, and their sum is a low-frequency amplitude modulated beam at a frequency of $|f1 - f2|$ that is detected by a photodiode. Referring back to Figure 2, the reference receiver sees $|f1 - f2|$ and the measure receiver sees $|f1 - (f2 + \Delta f)|$, where Δf is a Doppler shift in frequency caused by movement of the retroreflector. The laser axis board electronics compares the measure and reference frequencies, basically measuring to high accuracy the phase difference between them. For example, a phase change of 270° corresponds to a change in position of $270° \cdot (\lambda/2)/360° = 0.375\lambda = 237.3$ nm ($\lambda = 632.8$ nm, in air).

Error sources

Can we believe it when the interferometer reports position x.xxxxxx? Yes, when the machine, interferometer and compensation work well together. Machine design is a science and art; here we will only introduce key accuracy limitations for heterodyne interferometry.

Index of refraction in the measurement path

Assuming we are working in air, the vacuum wavelength of the source is multiplied by a 'Total Compensation Number' (*TCN*), where $TCN = (\eta_{air}/\eta_{vacuum})^{-1}$ plus an adjustment for thermal expansion of the part (for discussion later). This is a variable error proportional to the measurement distance. For example, a 10 ppb wavelength error produces a 10 nm error with the interferometer and mirror separated by one meter ($1 \text{ m} \cdot 10 \cdot 10^{-9}$ m/m). η_{air} is either measured directly or computed with the well-known Edlén equation [2]. Table 1 presents rules of thumb for estimating errors due to air temperature, pressure and humidity changes.

Table 1. Rules of thumb for error estimation.

Environmental change	Effect on TCN*
1°C increase in temperature	~1 ppm decrease
3 mm Hg increase in air pressure	~1 ppm increase
25% increase in relative humidity	~0.22 ppm decrease

* Values computed with the aid of "Refractive Index of Air Calculator Based on Modified Edlén Equation" [3].

Unlike temperature, pressure and humidity vary slowly. It is advisable to minimize temperature variation along the measurement path by managing air flow using baffles and air showers. Place heat-generating components away from the measurement beams whenever possible and make accommodations for heat removal. Temperature especially has a large effect on the measurement and stringent control is necessary.

Deadpath error

The laser system makes a relative measurement from an arbitrary zero point chosen by the designer. Referring to Figure 2, it is clear that the laser wavelength in both the reference and measurement paths is affected by index of refraction changes in the air. Referring to Figure 2, imagine putting the measurement corner cube the same distance away from the PBS as the reference corner cube, and calling this 'zero position'. Now assume the air temperature increases by 1°C causing a -1 ppm change in wavelength in both paths. Since the path lengths are equal, there is no net phase change at the measurement receiver and deadpath is zero in this case. As an example, assume 5 mm of deadpath in the reference arm and air temperature increase by 1°C. This causes a 1 ppm reduction in *TCN*, effectively 'shortening' the reference path and adding a +5 nm error to the measurement. Zero deadpath is the exception, even when operating in a vacuum, since the chamber thermal coefficient of expansion and the thermal coefficient of expansion of the interferometers themselves can affect the measurement and reference paths unequally. Deadpath only matters if the environmental conditions are changing between the time you reset position to zero and finish taking the measurement.

Laser source

The laser source is the heart of the system, and contributes a few error terms. Vacuum wavelength and wavelength stability show up as variable errors. Beam direction changes introduce a cosine error into the measurement. This is a lesser effect, caused for example by changes in the laser mounting due to thermal effects, and the mounting locations for all beam-bending and -splitting optics along the path, as well as the splitting and bending components themselves. Ellipticity and non-orthogonality of the two polarizations will add a cyclic error to the measurement, which is not proportional to the separation between the interferometer and retroreflector. This has been described in numerous papers [4].

Interferometer

Imperfect separation of *f1* and *f2* by the polarizing beam splitter causes a small amount of unintended mixing of the two polarizations that has been described and modeled in numerous papers on optical non-linearity, also called cyclic error. This is primarily a sinusoidal error having the same period as the fringes themselves. For example, a single-pass interferometer will have a fringe period of $\lambda/2$, a plane mirror (two-pass) unit has a period of $\lambda/4$.

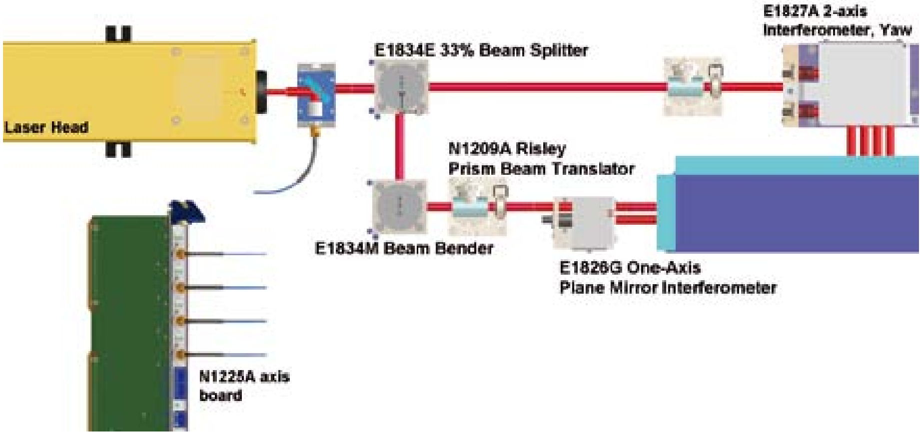

Application type: XY stage position measurement/control
Maximum stage velocity: 500 mm/s
Maximum stage travel: 200 mm in X, 50 mm in Y
Resolution: 0.15 nm
Environment: vacuum, 10^{-9} torr
Operating temperature: 22 ± 0.1°C
System materials: Invar (coefficient of thermal expansion = $1.5 \cdot 10^{-6}$ °C^{-1})
Position interface: VME
Measurement time: 20 minutes

Figure 3. Three-axis application example.

Mirrors

Mirrors contribute a fixed amount of reproducible error coming from their manufacturing process. A flatness specification of $\lambda/10$ measured at 635 nm implies 64 nanometers from peak to trough over the mirror surface that contributes a fixed error. The error can be reduced by mapping the mirror.

Example application

A sample configuration is shown in Figure 3. The XY stage operates in vacuum and is monitored for X and Y position. Interferometer E1827A measures mirror position at two points to track yaw. Hence, Z rotation is also monitored. Main components are the Agilent E1826EV and E1826FV interferometers, N1209A Risley prism translators, N1225A axis board, E1706C remote sensors and 5517DL laser head. Not shown in the figure: vacuum window, ST-ST fiber feedthrough, VME rack, power supplies and cables. The strain-free vacuum window with S-D 60-40 or better surface quality should provide transmitted wavefront distortion of < $\lambda/10$.

This application has three degrees of freedom and will use stage mirrors. Looking at error sources may give a rough idea of the best-case accuracy to expect; see Table 2.

Choosing the laser source

The Doppler shift from mirror motion in both directions has to be below the laser head split frequency and within the laser axis board frequency range. A two-pass interferometer produces one fringe per $\lambda/4$ travel distance. At 0.5 m/s, the Doppler shift from fringe motion is (0.5 m/s)/($\lambda/4$) = 3.16 MHz. The minimum input frequency for the laser axis board is 0.5 MHz, so the absolute minimum split frequency for the laser head is 3.66 MHz. The Agilent 5517DL split frequency is > 4.4 MHz, and this fits the velocity requirement. Assuming a 4.4 MHz split, the axis board will see from 1.24 to 7.6 MHz which fits well with its 0.5 to 30 MHz input frequency range.

References

[1] S. Cosijns, "Displacement laser interferometry with sub-nanometer uncertainty". Ph.D. thesis, Eindhoven University of Technology, 2004.
[2] B. Edlén, "The Refractive Index of Air". *Metrologia*, Vol.2, No.2, 71, 1966.
[3] Refractive Index of Air Calculator Based on Modified Edlén Equation. http://emtoolbox.nist.gov/Wavelength/Edlen.asp.
[4] N. Bobroff, "Residual errors in laser interferometry from air turbulence and nonlinearity". *Applied Optics* 26, 2676-2681, 1987.

Table 2. Error sources and magnitude.

Error source	Worst-case impact on X-axis measurement	Worst-case impact on Y-axis measurement
Laser head, 0.02 ppm wavelength accuracy with special calibration	± 4 nm error @ 200 mm	± 1 nm @ 50 mm
Laser head, 1 hour short-term wavelength stability 0.002 ppm	± 0.4 nm error @ 200 mm	± 0.1 nm @ 50 mm
Non-linearity error from interferometers	± 1 nm	± 1 nm
± 1 count error from digital electronics	± 0.15 nm	± 0.15 nm
Mirror quality ($\lambda/20$)*	± 16 nm	± 16 nm
Thermal coefficient of expansion for system materials	± 30 nm (over ± 0.1°C)	± 7.5 nm (over ± 0.1°C)
Interferometer thermal drift due to glass path imbalance	< 1 nm	< 1 nm

* Addition of redundant axes and mirror mapping can reduce this error.